Title

THE WEAKLY EXOTHERMIC REARRANGEMENT OF METHOXY RADICAL (CH3O') TO THE HYDROXYMETHYL RADICAL (CH2OH')

Author

Schaefer, H.F.

Publication Date

1982-09-01

Lawrence Berkeley Laboratory
UNIVERSITY OF CALIFORNIA

Materials & Molecular Research Division

Submitted to the Journal of Chemical Physics

THE WEAKLY EXOTHERMIC REARRANGEMENT OF METHOXY RADICAL ($CH_3O^{\cdot}$) TO THE HYDROXYMETHYL RADICAL ($CH_2OH^{\cdot}$)

Svein Saebø, Leo Radom, and Henry F. Schaefer III

September 1982

Prepared for the U.S. Department of Energy under Contract DE-AC03-76SF00098

DISCLAIMER

THE WEAKLY EXOTHERMIC REARRANGEMENT OF METHOXY RADICAL ($CH_3O^{\cdot}$) TO THE HYDROXYMETHYL RADICAL ($CH_2OH^{\cdot}$)

Svein SAEBØ and Leo RADOM

Research School of Chemistry, Australian National University, Canberra, A.C.T. 2600, Australia

Henry F. SCHAEFER III

Department of Chemistry and Lawrence Berkeley Laboratory, University of California, Berkeley, Ca 94720, and Research School of Chemistry, Australian National University, Canberra, A.C.T. 2600, Australia

[ABSTRACT]

Although the $CH_3O^{\cdot}$ and $CH_2OH^{\cdot}$ radicals have long been considered critical intermediates in combustion and atmospheric processes, only very recently has the potential significance of the isomerization $CH_3O^{\cdot} \rightarrow CH_2OH^{\cdot}$ been appreciated. This isomerization and related aspects of the $CH_3O^{\cdot}/CH_2OH^{\cdot}$ potential surface have been studied here using nonempirical molecular electronic structure theory with moderately large basis sets and with incorporation of electron correlation. The vibrational frequencies of $CH_3O^{\cdot}$, $CH_2OH^{\cdot}$ and seven other stationary points on the potential energy hypersurface have been predicted, both

to compare with results from spectroscopy and to provide estimates of zero-point vibrational corrections. In general, there is reasonable agreement with those vibrational frequencies of $CH_3O^{\cdot}$ and $CH_2OH^{\cdot}$ which are known from experiment. Our ab initio calculations predict that $CH_3O^{\cdot}$ lies 4.9 kcal mol^{-1} higher in energy than CH_2OH with a barrier to rearrangement to $CH_2OH^{\cdot}$ of 36.9 kcal mol^{-1}. Rearrangement of $CH_3O^{\cdot}$ to $CH_2OH^{\cdot}$ via a dissociation-recombination mechanism is energetically more costly (by 6.1 kcal mol^{-1}). The Jahn-Teller distortion of $CH_3O^{\cdot}$ from point group C_{3v} is described in some detail. Barriers to inversion and rotation in $CH_2OH^{\cdot}$ are predicted and compared with the results of ESR experiments. Finally the dissociation of $CH_3O^{\cdot}$ and $CH_2OH^{\cdot}$ to yield formaldehyde plus $H^{\cdot}$ are each predicted to involve modest reverse activation energies.

1. INTRODUCTION

The methoxy radical ($CH_3O^{\cdot}$) is widely agreed to play a major role in the oxidation of hydrocarbons, that is, in combustion chemistry.[1,2] $CH_3O^{\cdot}$ is likewise an important species in atmospheric chemistry.[3,4] However, due to the transient nature of this open-shell species, it is only in recent years that $CH_3O^{\cdot}$ has become the object of spectroscopic studies. Some of the most important such experimental investigations have involved electron spin resonance (ESR),[5] laser magnetic resonance (LMR),[6] electronic spectroscopy (UV absorption[7] and emission[8,9]), laser induced fluorescence,[10,11] and photodetachment[12,13] of the methoxy anion ($CH_3O^{\cdot}$). The methoxy radical has also received considerable theoretical attention,[14-21] its Jahn-Teller distortion from $\underline{C_{3v}}$ symmetry being of particular interest. The variety of modern spectroscopic techniques applied to $CH_3O^{\cdot}$ make it one of the most widely studied polyatomic organic free radicals. Nevertheless there is no experimental molecular structure for $CH_3O^{\cdot}$, although the spectroscopic studies provide support[7,8,10] for the large theoretically predicted[14] increase ($\sim$0.2Å) in the C-O distance upon electronic excitation. Moreover, only two of the ground-state vibrational frequencies are known experimentally, namely the symmetric umbrella motion[13] at ν_2=1325±30 cm^{-1} and the C-O stretch,[10] ν_3=1015 cm^{-1}.

Although less ubiquitous than $CH_3O^{\cdot}$, the hydroxymethyl radical ($CH_2OH^{\cdot}$) has been known for some time,[22-34] primarily as a result of ESR studies of the radiation of methanol, and is also thought to play some role in the chemistry of combustion[1] and of the atmosphere.[3]

The only spectroscopic studies of $CH_2OH^{\cdot}$, other than ESR, have been the matrix isolation work of Jacox and Milligan[35,36] and most recently the gas-phase LMR identification of Radford, Evenson and Jennings.[37] Of these, the recent paper by Jacox, exploiting the reaction between atomic fluorine and methanol, provides much insight into the structure and properties of the $CH_2OH^{\cdot}$ radical. Six or seven of the nine hydroxymethyl fundamental vibrational frequencies were observed, including the OH stretch (3650 cm^{-1}), the CO stretch (1183 cm^{-1}), and the torsion vibration (420 cm^{-1}). Assignments of the other observed fundamentals was attempted using the semiempirically predicted $CH_2OH^{\cdot}$ structure of Gordon and Pople[38] in concert with force constants derived from the vibrational spectra of six other isotopically substituted forms of $CH_2OH^{\cdot}$.

It has been known for at least twenty years that the radicals $CH_3O^{\cdot}$ and $CH_2OH^{\cdot}$ are nearly isoenergetic.[39-42] The early thermochemical data are summarized in the 1969 paper of Haney and Franklin,[42] who conclude that $CH_2OH^{\cdot}$ lies on the order of 5±5 kcal mol^{-1} below $CH_3O^{\cdot}$. In this light it struck us as surprising that until very recently the possibility and consequences of the unimolecular rearrangement

$$CH_3O^{\cdot} \rightarrow CH_2OH^{\cdot} \qquad (1)$$

had been discussed rarely if ever in the literature. However, Wendt and Hunziker[7] raised the possibility of reaction (1) in their 1977 study of the electronic spectrum of $CH_3O^{\cdot}$, noting that an exothermicity of 9 kcal mol^{-1} is obtained from the heats of formation given in the Handbook of Physics and Chemistry.[43]

Current interest in reaction (1) seems to stem largely from the 1980 paper of Radford. Radford[44] noted that the reaction

$$F^{\cdot} + CH_3OH \rightarrow CH_3O^{\cdot} + HF \qquad (2)$$

used as a source for methoxy radicals, also generated the LMR spectra of the $HO_2^{\cdot}$ radical. These $HO_2^{\cdot}$ LMR spectra could be intensified further by adding molecular oxygen (O_2) to the gas-flow system. Moreover during this process the $CH_3O^{\cdot}$ spectra remained at full intensity, consistent with the fact that the reaction

$$CH_3O^{\cdot} + O_2 \rightarrow HO_2^{\cdot} + CH_2O \qquad (3)$$

is known to be slow. Subsequently, Radford discovered that the source of the $HO_2^{\cdot}$ radicals was the hydroxymethyl radical reaction

$$CH_2OH^{\cdot} + O_2 \rightarrow HO_2^{\cdot} + CH_2O \qquad (4)$$

which he established to be much faster (rate coefficient about 3000 times greater) than the analogous methoxy reaction (3). As Radford noted, "this has importance for atmospheric chemistry, for if isomeric rearrangement of $CH_3O^{\cdot}$ to $CH_2OH^{\cdot}$ can occur even to a small extent, then the oxidation of $CH_3O^{\cdot}$ in the upper atmosphere may be governed by unimolecular isomerization rather than by the bimolecular reaction." (3).

In the absence of an experimental investigation of the methoxy isomerization (1), Batt, Burrows and Robinson[45] have estimated its exothermicity and rate coefficient from thermochemical considerations.[46] In this manner, they deduce a value of 7.5 kcal mol^{-1} for the activation energy. Assuming these estimates are correct, Batt, Burrows and Robinson conclude that although the methoxy radical isomerization may

not play an important role in atmospheric chemistry, at the elevated temperatures associated with combustion, reaction (1) could be important.

We present here a systematic theoretical study of the isomers $CH_3O^{\cdot}$ and $CH_2OH^{\cdot}$, of the transition structure for their interconversion, and of their separate dissociations to $H^{\cdot}$ + formaldehyde. Although previous ab initio studies of $CH_3O^{\cdot}$[14-19] and $CH_2OH^{\cdot}$[15,47-49] have been reported, it is only since completion of the present study that we have become aware of two independent investigations[20,21] of the rearrangement and dissociative processes involving $CH_3O^{\cdot}$ and $CH_2OH^{\cdot}$. A brief comparison of our results with those of ref. 20 is included below and some discrepancies noted and discussed. Insufficient information is available to allow a detailed analysis of the results of ref. 21.

II. THEORETICAL APPROACH

Ab initio calculations at seven distinct levels of theory were carried out using a modified version[50] of the Gaussian 80 system of programmes.[51] Three of these, corresponding to basis sets of increasing size, lie within the unrestricted Hartree-Fock approximation[52] and were used in conjunction with analytical gradient methods[53] to obtain optimized geometrical structures. The basis sets used were the split-valence 3-21G set,[54] the split-valence plus d-polarization 6-31G* set,[55] and the split-valence plus dp-polarization 6-31G** set.[55] Harmonic vibrational frequencies were routinely obtained for all stationary points at the HF/3-21G level. These served firstly to characterize minima (all real frequencies) and saddle points (one

imaginary frequency) in the surface, and secondly to allow the determination of zero-point vibrational energies. For the $CH_3O^{\cdot}$ and $CH_2OH^{\cdot}$ equilibrium structures, the vibrational frequencies were also obtained at the HF/6-31G* level of theory.

In order to obtain improved energy comparisons, additional calculations were performed on the HF-optimized structures with electron correlation incorporated through second- and third-order Møller-Plesset perturbation theory.[56,57] We use the notation MP3/6-31G**//6-31G**, for example, to indicate a third-order Møller-Plesset calculation with the 6-31G** basis set on a structure optimized at the HF/6-31G** level.

III. RESULTS AND DISCUSSION

A. The Jahn-Teller Distortion in $CH_3O^{\cdot}$

The present theoretical study of the $CH_3O^{\cdot}$ Jahn-Teller problem included consideration of the degenerate $\underline{C}_{3\underline{v}}$ state:

$$1a_1^2\ 2a_1^2\ 3a_1^2\ 4a_1^2\ 1e^4\ 5a_1^2\ 2e^3 \qquad {}^2E \qquad (5)$$

and the two distorted $\underline{C}_{\underline{s}}$ states:

$$1a'^2\ 2a'^2\ 3a'^2\ 4a'^2\ 1a''^2\ 5a'^2\ 6a'^2\ 2a''^2\ 7a' \qquad {}^2A' \qquad (6)$$

$$1a'^2\ 2a'^2\ 3a'^2\ 4a'^2\ 1a''^2\ 5a'^2\ 6a'^2\ 7a'^2\ 2a'' \qquad {}^2A'' \qquad (7)$$

The geometrical structures of $\underline{C}_{3\underline{v}}$-constrained methoxy radical ($\underset{\sim}{1}$) and of the two states ($\underset{\sim}{2}$,$\underset{\sim}{3}$) where the symmetry is reduced to $\underline{C}_{\underline{s}}$ are included in Table I. For reference, the key features of the 6-31G**

structures are qualitatively sketched in Figure 1.

The structures show, in accordance with the early prediction of Yarkony,[14] that the Jahn-Teller distortion is relatively small. The OCH angles, all three of which are, of course, the same in point group $\underline{C_{3v}}$, change from 109.9° to 106.1° (one of these) and 111.7° (two of these) for the $^2A'$ form ($\underset{\sim}{2}$) and to 112.8° (one of these) and 108.4° (two of these) for the $^2A''$ form ($\underset{\sim}{3}$) at the HF/6-31G** level of theory. Our frequency calculations show that both the $\underline{C_s}$-constrained forms ($^2A'$ and $^2A''$) are true minima on the 3-21G potential energy hypersurface. Comparison of the $^2A'$ and $^2A''$ geometries shows that the changes from the $\underline{C_{3v}}$ structure are small and in opposite directions, as expected for the two components of a Jahn-Teller degenerate ground state like $CH_3O^{\cdot}$.

In general, the 3-21G, 6-31G* and 6-31G** structures for $CH_3O^{\cdot}$ are in good accord. However, the C-O distance is an exception, there being a reduction of 0.06Å in going from 3-21G to 6-31G*. The HF/6-31G** result (1.382Å) is in reasonable agreement with the perturbation theory result of Adams, Bent, Purvis and Bartlett[18a] and with Jackel's recent CI prediction,[19] both 1.405Å. As expected, the HF/3-21G C-O distance of 1.444 Å agrees well with the DZ SCF prediction (1.44Å) of Yarkony.[14]

The total and relative energies for the three $CH_3O^{\cdot}$ forms are given in Table II. All seven levels of theory predict a small energy lowering (0.21 - 0.63 kcal mol^{-1}) when the methoxy radical undergoes its Jahn-Teller distortion from $\underline{C_{3v}}$ symmetry. At the HF/6-31G** level, there is a Jahn-Teller stabilization of 0.43 kcal mol^{-1}; this increases

slightly to 0.63 kcal mol^{-1} when electron correlation is incorporated at the MP3/6-31G** level. The $^2A''$ state lies very slightly above $^2A'$ at all levels of theory with the splitting varying from 0.04-0.12 kcal mol^{-1}. Our best results (0.56 kcal mol^{-1} Jahn-Teller stabilization and 0.12 kcal mol^{-1} Jahn-Teller splitting) agree well with the very recent results of Bent et al.[18b] from many-body perturbation theory calculations (0.64 and 0.17 kcal mol^{-1}, respectively). We note in contrast that Adams, Bartlett and Purvis[20] appear to have considered only the higher energy $^2A''$ state (3) in their study of unimolecular reactions involving $CH_3O^{\cdot}$ and $CH_2OH^{\cdot}$.

B. Equilibrium Structure and Internal Rotation and Inversion in $CH_2OH^{\cdot}$

We present here the first complete set of theoretical predictions for the $CH_2OH^{\cdot}$ rotation-inversion potential energy hypersurface. This aspect of the $CH_3O^{\cdot}$ energy surface involves some subtleties, as may be seen from Figure 2. In terms of specific bond distances and bond angles, there is only a single distinct equilibrium geometry of connectedness $CH_2OH^{\cdot}$ (4). However, Figure 2 shows that upon inversion at the carbon center the structure 4a becomes 4b and the two are not superposable when H_1 and H_2 are distinguished by labels, i.e. they are optical isomers (enantiomers). Moreover, there is a second transition structure for interconversion of equivalent $CH_2OH^{\cdot}$ structures, and this involves internal rotation about the C-O bond. Figure 2 shows that this rotational transition structure connects 4a with 4c which is neither superposable with 4a nor an enantiomer of 4a. When appropriately labelled, 4a and 4c may be distinguished as synclinal-anticlinal rotational isomers.[58] The details of these isomerizations have not been fully addressed in earlier discussions[30,32,48] which emphasize the rotation about the C-O bond.

Theoretical geometries for $CH_2OH^{\cdot}$ ($\underset{\sim}{4}$) and for the inversion ($\underset{\sim}{5}$) and rotation ($\underset{\sim}{6}$) transition structures are sketched in Figure 1, with detailed data given in Table I. The $CH_2OH^{\cdot}$ equilibrium structure is found to be completely asymmetric (i.e. of C_1 symmetry). Our vibrational analysis at the 3-21G and 6-31G* levels confirms that this structure is a minimum in the potential energy surface. In contrast, Adams et al.[20] report a structure of C_s symmetry for $CH_2OH^{\cdot}$. Their structure is almost identical to our rotational transition structure ($\underset{\sim}{6}$) and, with one imaginary frequency, this is clearly not a minimum in the surface. Apart from the inversion and torsional aspects, our predicted geometries for the inversion and internal rotation transition structures are quite similar to that of the equilibrium structure $\underset{\sim}{4}$.

The predicted barrier heights for inversion and rotation are presented in Table III. Experimental analyses[30,32] of the ESR spectra of $CH_2OH^{\cdot}$ have assumed the inversion barrier to be negligible compared to the barrier for rotation. In this manner, Hudson[30] and Krusik, Meakin and Jesson[32] obtain barrier heights of 2.3 and $\sim$4 kcal mol^{-1}, respectively. We find barriers to rotation of 2.75 kcal mol^{-1} at the HF/6-31G** level and 3.90 kcal mol^{-1} (MP3/6-31G**) when correlation is taken into account. Corresponding calculated inversion barriers are 1.15 (HF/6-31G**) and 0.92 (MP3/6-31G**) kcal mol^{-1}. Our best results thus show (Figure 3) that the barrier to inversion is indeed considerably smaller than the barrier to internal rotation.

C. Vibrational Frequencies of $CH_3O^{\cdot}$ and $CH_2OH^{\cdot}$

The vibrational frequencies for all species were calculated by numerical differentiation of the energy gradient at the optimized geometries. In order to obtain accurate analytical gradients, a high degree of convergence in the SCF procedure is required. Our standard requirement for vibrational frequency calculations is a convergence in the density matrix of 10^{-7}. For the methoxy radical, however, convergence problems were experienced and we were forced to relax this convergence criterion to 10^{-5}. To test the effect of this change on the calculated frequencies, the vibrational frequencies of methanol were obtained with both convergence criteria. As a consequence of relaxing the convergence from 10^{-7} to 10^{-5}, the low frequency torsional mode changed by 14 cm^{-1}; however, for all the remaining modes, the changes were less than 5 cm^{-1}. The zero-point vibrational energy was unaffected. We assume that our use of the 10^{-5} density matrix convergence results in calculated vibrational frequencies for the methoxy radical with an accuracy similar to that of methanol, which is quite satisfactory for our purposes here. All the remaining vibrational frequency calculations in this study were carried out with our standard convergence criterion.

In discussing the infrared spectral results for $CH_2OH^{\cdot}$ and $CH_3O^{\cdot}$, it is helpful to have at hand the known vibrational frequencies of methanol (CH_3OH)[59] from which both radicals may be formally derived by removal of a hydrogen atom. Table IV shows a comparison of the harmonic frequencies predicted at the HF/3-21G and HF/6-31G* levels of theory with reported experimental frequencies. For methanol, for which the experimental frequencies are well established, the predicted

harmonic frequencies are each higher than the corresponding experimental values. Such behaviour is quite general[60,61] and the deviations from experiment are due both to neglect of electron correlation and to the neglect of anharmonicity in the theoretical predictions. If the 6-31G* frequencies are scaled by a factor of 0.9, the differences between the theoretical and experimental frequencies are less than 25 cm^{-1} for all modes except the a" CH_3 stretch for which the discrepancy is 52 cm^{-1}.

Similar scaling of the 6-31G* frequencies for $CH_2OH^{\cdot}$ and $CH_3O^{\cdot}$ produces satisfactory agreement with the known experimental frequencies with the exception of the observed frequency at 569 cm^{-1} for $CH_2OH^{\cdot}$ for which the theoretically predicted value is about 200 cm^{-1} too high. The unusually high C-O stretching frequency in $CH_2OH^{\cdot}$ observed both experimentally (1183 cm^{-1}) and theoretically (scaled value 1158 cm^{-1}) is worth noting. Included in Table IV are 3-21G frequencies for both $^2A'$ ($\underset{\sim}{2}$) and $^2A''$ ($\underset{\sim}{3}$) states of $CH_3O^{\cdot}$. Most frequencies are very similar for the two states, the only exception being the two CH_3 rocking vibrations. These are, of course, the frequencies most intimately connected with the Jahn-Teller distortions and it is not surprising that the distortion in the two directions leads to opposite orderings of the a' and a" CH_3 rock vibrations.

Bent et al.,[18b] in a partial vibrational analysis, have obtained theoretical frequencies for the CH_3 "degenerate" stretch, deformation (bend) and rock. Their calculated frequencies (2314; 1066; 792 cm^{-1}) are all substantially smaller than our corresponding pairs of values (3254, 3277; 1691, 1642; 1158, 1210 cm^{-1}). The reason for the

discrepancy is not clear but our frequencies look eminently reasonable if we compare also with the corresponding values (3294, 3217; 1698, 1686; 1152, 1254 cm^{-1}) for methanol.

The calculated harmonic vibrational frequencies, in addition to being of some interest in their own right and to allowing stationary points in the $CH_3O^{\cdot}$ surface to be characterized as minima or saddle points, also allow the evaluation of zero-point vibrational energies. These are listed in Table V and may be used to correct calculated reaction energies and barrier heights for the effects of zero-point vibrations. As noted above and elsewhere,[60,61] vibrational frequencies at the HF/3-21G and HF/6-31G* levels are generally overestimated by about 10%. Accordingly, the calculated zero-point energies are scaled by 0.9 when used in the evaluation of reaction energies and barrier heights in this paper.

D. Relative Stabilities of Methoxy and Hydroxymethyl Radicals

Relative energies of the methoxy (2) and hydroxymethyl (4) radicals are listed in Table VI. At the Hartree-Fock level of theory, $CH_3O^{\cdot}$ is predicted to lie lower in energy. However, when electron correlation is taken into account, $CH_2OH^{\cdot}$ drops below $CH_3O^{\cdot}$ with our best estimate (MP3/6-31G**//6-31G** plus zero-point vibrational correction) of the energy difference being 4.9 kcal mol^{-1}. This may be compared with a 7.5 kcal mol^{-1} thermochemical estimate of Batt, Burrows and Robinson[45] and with an estimate of 4 kcal mol^{-1} resulting from a recent redetermination[13] of the heat of formation of the methoxy radical. Adams et al.[20] find an energy difference of 3.9 kcal mol^{-1} at the SDQ MBPT(4) level without zero-point correction in apparent excellent agreement with our raw

MP3/6-31G** result (3.8 kcal mol^{-1}). However, as noted above, their $CH_2OH^{\cdot}$ geometry corresponds to the rotational transition structure (6) and would thus be expected to be too high in energy by about 4 kcal mol^{-1}. Harding[21] reports an energy difference between 2 and 4 of 2 kcal mol^{-1} from POL-CI calculations.

E. The Intramolecular $CH_3O^{\cdot} \rightarrow CH_2OH^{\cdot}$ Rearrangement

As noted above, the $CH_3O^{\cdot} \rightarrow CH_2OH^{\cdot}$ rearrangement is predicted to be exothermic by 4.9 kcal mol^{-1}. The determination of the transition structure and barrier height is of course necessary to assess whether or not this is a facile process. The 6-31G** transition structure (7) has C_s symmetry and is sketched in Figure 1, with complete geometrical parameters for all three levels of theory given in Table I. For the triplet diradical system with one less electron

$$CH_3\dot{N}\cdot \rightarrow \dot{C}H_2NH \qquad (8)$$

a plane of symmetry is also found in the transition structure.[62] In fact, other features of the $CH_3O^{\cdot} \rightarrow CH_2OH^{\cdot}$ transition structure are also quite similar to those predicted for the triplet methylnitrene rearrangement (8). In both cases, the migrating hydrogen atom forms a roughly equilateral triangle with bond lengths in the order r(C-X) > r(C-H) > r(X-H), where X=C for reaction (1) and X=N for reaction (8). Table I shows that at each of the three levels of theory used for geometry optimization, the C-O length in $CH_2OH^{\cdot}$ is less than that for the reactant $CH_3O^{\cdot}$ radical (by 0.015Å with 6-31G**), with the C-O length in the transition structure lying somewhere in between. In this sense, the transition structure is certainly intermediate between reactant $CH_3O^{\cdot}$ and product $CH_2OH^{\cdot}$. The only other especially noteworthy

aspect of the present structural predictions is the large difference (0.071Å) between the 3-21G and 6-31G** predictions of the C-O distance in the transition structure.

Barrier heights for the isomerization are included in Table VI. The predicted barrier heights follow the general pattern, as a function of level of theory, found previously for 1,2-hydrogen shifts.[62-66] That is, both the addition of polarization functions and the treatment of correlation effects serve to lower the predicted barrier height. If trends in changes predicted[65,66] in going to still higher levels of theory for the $H_2CO \rightarrow H_2+CO$ and $H_2CC: \rightarrow HCCH$ rearrangements also hold for reaction (1), then we might expect the barrier to be slightly lower than our best estimate of 36.1 kcal mol^{-1}. Batt[45] has empirically estimated a barrier of 26.1 kcal mol^{-1}. Barriers calculated by Adams et al.[20] and by Harding[21] are 35.6 and 37 kcal mol^{-1}, respectively, before correction for zero-point vibrations.

F. Dissociative Reactions of $CH_3O^{\cdot}$ and $CH_2OH^{\cdot}$

An alternative mechanism for isomerization of $CH_3O^{\cdot}$ to $CH_2OH^{\cdot}$ would involve dissociation and recombination. For this reason, we examined the two dissociation reactions

$$CH_3O^{\cdot} \rightarrow CH_2O + H^{\cdot} \qquad (9)$$

and

$$CH_2OH^{\cdot} \rightarrow CH_2O + H^{\cdot} \qquad (10)$$

The predicted transition structures are displayed in Figure 1 (schematic) and Table I (detailed). As expected, the transition structures for (9) and (10) have long C---H (1.843Å) and O---H (1.479Å) bonds, respectively.

The barriers for the reverse of reactions (9) and (10), i.e. for the addition of H$^{\cdot}$ to the C or O, respectively, of formaldehyde, are presented in Table VII. At all levels of theory, a smaller barrier is predicted for addition to C than to O with our best estimates being 12.4 and 20.1 kcal mol^{-1} respectively.

G. Comparative Aspects of the $CH_3O^{\cdot}/CH_2OH^{\cdot}$ Potential Energy Surface

A schematic energy profile for key aspects of the $CH_3O^{\cdot}/CH_2OH^{\cdot}$ potential energy surface is presented in Figure 4. The transition structure for intramolecular rearrangement (7) lies at 41.0 kcal mol^{-1} relative to $CH_2OH^{\cdot}$ (4) while the transition structures (8,9) for dissociation from $CH_3O^{\cdot}$ and $CH_2OH^{\cdot}$ lie at 39.4 kcal mol^{-1} and 47.1 kcal mol^{-1}, respectively. Adams et al.[20] reported energies relative to $CH_2OH^{\cdot}$ of 39.5, 39.1 and 47.8 kcal mol^{-1} for 7, 8 and 9 respectively, before zero-point corrections. Thus it is slightly easier (by 1.6 kcal mol^{-1}) to remove a hydrogen atom from $CH_3O^{\cdot}$ than to isomerize to $CH_2OH^{\cdot}$. However, isomerization via dissociation-recombination would need to surmount the barrier at 9 (47.1 kcal mol^{-1}) and such a process is thus predicted to be 6.1 kcal mol^{-1} more costly than intramolecular rearrangement.

IV. CONCLUDING REMARKS

The present theoretical study predicts that the hydroxymethyl radical (4) lies 4.9 kcal mol^{-1} lower in energy than the methoxy radical (2). The favored mode of isomerization of $CH_3O^{\cdot}$ to $CH_2OH^{\cdot}$ is intramolecular rearrangement (requiring 36.1 kcal mol^{-1}) rather than

dissociation-recombination (requiring 42.2 kcal mol^{-1}). Predicted activation energies of the type reported here are notoriously high[67] with errors of 5 kcal mol^{-1} being typical. Nevertheless, the energetics reported here, especially if taken with this empirical observation in mind, should be of value in future discussions of these important combustion species. Furthermore, it is hoped that the predicted vibrational frequencies of $CH_3O^{\cdot}$ and $CH_2OH^{\cdot}$ will stimulate further spectroscopic studies.

ACKNOWLEDGEMENTS

One of us (HFS) was supported by the U.S. Department of Energy under Contract Number DE-AC03-76SF00098 and the U.S. National Science Foundation.

[REFERENCES]

1. See Volumes I, II, and III of Oxidation of Organic Compounds, Advances in Chemistry Series (American Chemical Society, Washington, D.C., 1968)

2. K.L. Demerjian, J.A. Kerr, and J.G. Calvert, Adv. Environ. Sci. Technol., 4, 1 (1974)

3. J. Heicklen, Atmospheric Chemistry (Academic Press, New York, 1976)

4. J.T. Herron, R.E. Huie, and J.A. Hodgeson, editors, Chemical Kinetic Data Needs for Modeling the Lower Troposphere, Natl. Bur. Stand. (U.S.) Spec. Publ. 557 (U.S. GPO, Washington, D.C., 1979)

5. M. Iwasaki and K. Toriyama, J. Amer. Chem. Soc. 100, 1964 (1978).

6. H.E. Radford and D.K. Russell, J. Chem. Phys., 66, 2222 (1977); D.K. Russell and H.E. Radford, J. Chem. Phys., 72, 2750 (1980)

7. H.R. Wendt and H.E. Hunziker, J. Chem. Phys., 71, 5202 (1979)

8. K. Ohbayashi, H. Akimoto, and I. Tanaka, J. Phys. Chem., 81, 798 (1977)

9. M. Sutoh, N. Washida, H. Akimoto, M. Nakamura, and M. Okuda, J. Chem. Phys., 73, 591 (1980)

10. G. Inoue, H. Akimoto, and M. Okuda, (a) Chem Phys. Lett., 63, 213 (1979); (b) J. Chem. Phys., 72, 1769 (1980)

11. (a) N. Sanders, J.E. Butler, L.R. Pasternack, and J.R. McDonald, Chem. Phys., 49, 17 (1980); (b) D.E. Powers, J.B. Hopkins, and R.E. Smalley, J. Phys. Chem., 85, 2711 (1981)

12. K.J. Reed and J.I. Brauman, J. Amer. Chem. Soc., 97, 1625 (1975); B.K. Janousek, A.H. Zimmerman, K.J. Reed, and J.I. Brauman, J. Amer. Chem. Soc., 100, 6142 (1978)

13. P.C. Engelking, G.B. Ellison, and W.C. Lineberger, J. Chem. Phys., 69, 1826 (1978)

14. D.R. Yarkony, H.F. Schaefer, and S. Rothenberg, J. Amer. Chem. Soc., 96, 656 (1974)

15. W.A. Lathan, L.A. Curtiss, W.J. Hehre, J. B. Lisle, and J.A. Pople, Progr. Phys. Org. Chem., 11, 175 (1974)

16. H. Umeyama and S. Nakagawa, Chem. Pharm. Bull. 25, 1671 (1977)

17. J.T. Hougen, J. Mol. Spectroscopy, 81, 73 (1980)

18. (a) G.F. Adams, G.D. Bent, G.D. Purvis and R.J. Bartlett, Chem. Phys. Lett., 81, 461 (1981);
(b) G.D. Bent, G.F. Adams, R.H. Bartram, G.D. Purvis and R.J. Bartlett, J. Chem. Phys., 76, 4144 (1982)

19. C.F. Jackels, J. Chem. Phys. 76, 505 (1982)

20. G.F. Adams, R.J. Bartlett and G.D. Purvis, Chem. Phys. Lett., 87, 311 (1982)

21. L.B. Harding in Annual Report, Theoretical Chemistry Group (Argonne National Laboratory, 1982)

22. M. Fujimoto and D.J.E. Ingram, Trans. Faraday Soc., 54, 1304 (1958)

23. M.C.R. Symons, J. Chem. Soc., 277 (1959)

24. W.T. Dixon and R.O.C. Norman, J. Chem. Soc. 3119 (1963)

25. H. Fischer, Mol. Phys. 9, 149 (1965)

26. R. Livingston and H. Zeldes, J. Chem. Phys., 44, 1245 (1966); 45, 1946 (1966)

27. J.Q. Adams, J. Amer. Chem. Soc., 90, 5363 (1968)

28. M. McMillan and R.O.C. Norman, J. Chem. Soc. B 590 (1968)

29. R. Poupko and O. Lowenstein, J. Chem. Soc. A 949 (1968)

30. A. Hudson, J. Chem. Soc. A 2513 (1969)

31. E.L. Cochran, F.J. Adrian, and V.A. Bowers, J. Phys. Chem., 74, 2083 (1970)

32. P.J. Kusic, P. Meakin, and J.P. Jesson, J. Phys. Chem., 75, 3438 (1971)

33. A.J. Dobbs, B.C. Gilbert, and R.O.C. Norman, J. Chem. Soc. A 124 (1971)

34. F. Dainton, I. Janovsky, and G.A. Salmon, Proc. Roy. Soc. (London) A327, 305 (1972)

35. M.E. Jacox and D.E. Milligan, J. Mol. Spectroscopy, 47, 148 (1973)

36. M.E. Jacox, Chem. Phys., 59, 213 (1981)

37. H.E. Radford, K.M. Evenson, and D.A. Jennings, Chem. Phys. Lett., 78, 589 (1981)

38. M.S. Gordon and J.A. Pople, J. Chem. Phys., 49, 4643 (1968)

39. E. Buckley and E. Whittle, Trans. Faraday Soc., 58, 536 (1962)

40. J.A. Kerr, Chem. Rev., 66, 465 (1966)

41. R. Shaw and J.C.J. Thynne, Trans. Faraday Soc., 62, 104 (1966)

42. M.A. Haney and J.L. Franklin, Trans. Faraday Soc., 65, 1794 (1969)

43. R.C. Weast, Handbook of Physics and Chemistry, 59th edition (Chemical Rubber, Cleveland, 1978), p F245

44. H.E. Radford, Chem. Phys. Lett., 71, 195 (1980)

45. L. Batt, J.P. Burrows and G.N. Robinson, Chem. Phys. Lett., 78, 467 (1981)

46. For general guidelines, see S.W. Benson, Thermochemical Kinetics, (Wiley, New York, 1976)

47. G.L. Bendalozzi, P. Palmieri, and G.F. Pedulli, Chem. Phy. Lett. 29, 123 (1974)

48. T.K. Ha, Chem. Phys. Lett., 30, 379 (1975)

49. M.-H. Whangbo, S. Wolfe, and F. Bernardi, Can. J. Chem., 53, 3040 (1975)

50. L. Farnell and R.H. Nobes, unpublished

51. J.S. Binkley, R.A. Whiteside, R. Krishnan, R. Seeger, D.J. DeFrees, H.B. Schlegel, S. Topiol, L.R. Khan, and J.A. Pople, QCPE, 13, 406 (1981)

52. J.A. Pople and R.K. Nesbet, J. Chem. Phys., 22, 571 (1954)

53. D. Poppinger, Chem. Phys. Lett., 34, 352 (1975); 35, 550 (1975)

54. J.S. Binkley, J.A. Pople, and W.J. Hehre, J. Amer. Chem. Soc., 102, 939 (1980)

55. P.C. Hariharan and J.A. Pople, Theoret. Chim. Acta., 28, 213 (1973)

56. C. Møller and M.S. Plesset, Phys. Rev., 46, 618 (1934)

57. J.A. Pople, J.S. Binkley and R. Seeger, Int. J. Quantum, Chem. Symp., 10, 1 (1976)

58. For a description of this notation, see pages 68-69 of M. Hanack, Conformation Theory (Academic Press, New York, 1965)

59. W.J. Hehre, unpublished data

60. P. Pulay in Volume 4, Modern Theoretical Chemistry, editor H.F. Schaefer (Plenum, New York, 1977)

61. J.A. Pople, H.B. Schlegel, R. Krishnan, D.J. De Frees, J.S. Binkley, M.J. Frisch, R.A. Whiteside, R.F. Hout and W.J. Hehre, Int. J. Quantum Chem. Symp., 15, 269 (1981)

62. J. Demuynck, D.J. Fox, Y. Yamaguchi and H.F. Schaefer, J. Amer. Chem. Soc., 102, 6204 (1980)

63. H.F. Schaefer, Accounts Chem. Res., 12, 288 (1979)

64. R.H. Nobes, L. Radom and W.R. Rodwell, Chem. Phys. Lett., 74, 269 (1980)

65. M.J. Frisch, R. Krishnan and J.A. Pople, J. Phys Chem., 85, 1467 (1981)

66. R. Krishnan, M.J. Frisch, J.A. Pople and P.v.R. Schleyer, Chem. Phys. Lett., 79, 408 (1981)

67. J.D. Goddard, Y. Yamaguchi and H.F. Schaefer, J. Chem. Phys., 75, 3459 (1981)

TABLE I. Optimized (UHF) geometrical parameters for stationary points on the $CH_3O^{\cdot}$ potential energy hypersurface.[a,b]

$\underset{\sim}{1}$ $CH_3O^{\cdot}$ ($\underline{C}_{3_{\underline{V}}}$, ^2E)

Parameter	3-21G	6-31G*	6-31G**
r(C-H)	1.082	1.086	1.087
r(C-O)	1.447	1.385	1.386
<OCH	109.5	109.8	109.9
<HCH[c]	109.5	109.1	109.1

$\underset{\sim}{2}$ $CH_3O^{\cdot}$ ($\underline{C}_{\underline{S}}$, $^2A'$)

Parameter	3-21G	6-31G*	6-31G**
$r(C-H_1)$	1.081	1.085	1.086
$r(C-H_3)$	1.085	1.088	1.089
r(C-O)	1.444	1.383	1.382
$<OCH_1$	111.2	111.6	111.7
$<OCH_3$	106.0	106.0	106.1
$<H_1CH_2$	110.6	110.5	110.5
$<H_1CH_3$	108.9	108.5	108.3

$\underset{\sim}{3}$ $CH_3O^{\cdot}$ ($\underline{C}_s$, $^2A''$)

Parameter	3-21G	6-31G*	6-31G**
$r(C\text{-}H_1)$	1.083	1.087	1.087
$r(C\text{-}H_3)$	1.081	1.085	1.086
$r(C\text{-}O)$	1.445	1.383	1.383
$<OCH_1$	108.0	108.3	108.4
$<OCH_3$	112.3	112.7	112.8
$<H_1CH_2{}^c$	108.2	107.7	107.6
$<H_1CH_3$	110.1	109.8	109.8

$\underset{\sim}{4}$ $CH_2OH^{\cdot}$ ($\underline{C}_1$)

Parameter	3-21G	6-31G*	6-31G**
$r(C\text{-}H_1)$	1.075	1.078	1.078
$r(C\text{-}H_2)$	1.069	1.073	1.074
$r(C\text{-}O)$	1.392	1.359	1.357
$r(O\text{-}H)$	0.964	0.946	0.943
$<OCH_1$	119.0	117.7	117.9
$<OCH_2$	112.8	112.7	113.0
$<H_1CH_2{}^c$	119.7	118.7	118.9
$<COH$	112.2	110.2	110.4
$<H_1COH$	-35.0	-33.8	-33.3
$<H_2COH$	177.2	182.3	181.9

$\underset{\sim}{5}$ $CH_2OH^{\cdot}$ ($\underline{C_s}$, Inversion Transition Structure)

Parameter	3-21G	6-31G*	6-31G**
$r(C\text{-}H_1)$	1.070	1.071	1.072
$r(C\text{-}H_2)$	1.066	1.068	1.069
r(C-O)	1.389	1.357	1.356
r(O-H)	0.964	0.946	0.942
$<OCH_1$	121.3	120.6	120.5
$<OCH_2$	114.8	115.5	115.5
$<H_1CH_2{}^c$	123.9	123.9	124.0
<COH	112.5	110.4	110.5

$\underset{\sim}{6}$ $CH_2OH^{\cdot}$ ($\underline{C_s}$, Rotation Transition Structure)

Parameter	3-21G	6-31G*	6-31G**
$r(C\text{-}H_1)$	1.073	1.076	1.077
r(C-O)	1.400	1.367	1.365
r(O-H)	0.967	0.948	0.944
$<OCH_1$	117.0	116.3	116.5
<COH	112.1	110.5	110.7
$<H_1CH_2{}^c$	120.0	119.2	119.3
$<H_1COH$	103.0	105.8	104.8
$<OCH_{12}{}^d$	24.8	28.8	28.0

$\underset{\sim}{7}$ Transition Structure: $CH_3O^{\cdot} \rightarrow CH_2OH^{\cdot}$ ($\underline{C_s}$)

Parameter	3-21G	6-31G*	6-31G**
$r(C\text{-}H_1)$	1.072	1.078	1.079
$r(C\text{-}O)$	1.439	1.368	1.367
$r(O\text{-}H)^c$	1.212	1.186	1.186
$r(C\text{-}H)$	1.330	1.277	1.265
$<OCH_1$	116.8	117.2	117.3
$<OCH$	51.7	53.1	53.4
$<COH^c$	59.5	59.5	58.9
$<H_1CH_2$	119.7	118.4	118.2

$\underset{\sim}{8}$ Transition Structure: $CH_3O^{\cdot} \rightarrow CH_2O{+}H^{\cdot}$ ($\underline{C_s}$)

Parameter	3-21G	6-31G*	6-31G**
$r(C\text{-}H_1)$	1.078	1.086	1.087
$r(C\text{-}H_3)$	2.019	1.832	1.843
$r(C\text{-}O)$	1.259	1.226	1.226
$<OCH_1$	121.4	121.1	121.1
$<OCH_3$	100.3	99.7	99.6
$<H_1CH_2{}^c$	116.6	116.8	116.8
$<H_1CH_3$	88.2	90.1	90.0

$\underset{\sim}{9}$ Transition Structure: $CH_2OH^{\cdot} \rightarrow CH_2O+H^{\cdot}$ ($\underline{C}_s$)

Parameter	3-21G	6-31G*	6-31G**
$r(C-H_1)$	1.075	1.081	1.083
$r(C-O)$	1.287	1.255	1.251
$r(O-H)$	1.570	1.461	1.479
$\angle OCH_1$	120.8	120.5	120.6
$\angle H_1CH_2$ [c]	118.3	118.8	118.6
$\angle COH$	115.1	115.7	115.9
$\angle H_1COH$	88.0	87.3	87.7

[a] See Figure 1 for atom numbering

[b] All bond lengths in angstroms, bond angles in degrees

[c] A non-independent parameter

[d] H_{12} denotes a point on the bisector of H_1CH_2

TABLE II. Total energies[a] (hartrees), Jahn-Teller stabilizations[b] (kcal mol^{-1}) and Jahn-Teller splittings[c] (kcal mol^{-1}) for $CH_3O^{\cdot}$.

Method	Total Energy[a]	Jahn-Teller Stabilization[b]	Jahn-Teller Splitting[c]
3-21G//3-21G	-113.79195	0.35	0.06
6-31G*//6-31G*	-114.42075	0.42	0.08
6-31G**//6-31G**	-114.42558	0.43	0.08
MP2/6-31G**//6-31G*	-114.70967	0.63	0.14
MP2/6-31G**//6-31G**	-114.70971	0.63	0.14
MP3/6-31G**//6-31G*	-114.73318	0.57	0.13
MP3/6-31G**//6-31G**	-114.73320	0.56	0.12

a $E(\underset{\sim}{2})$

b $E(\underset{\sim}{1}) - E(\underset{\sim}{2})$

c $E(\underset{\sim}{3}) - E(\underset{\sim}{2})$

TABLE III. Total energies (hartrees), inversion barriers (kcal mol^{-1}) and rotational barriers (kcal mol^{-1}) for $CH_2OH^{\cdot}$.

Method	Total Energy[a]	Inversion[b] Barrier	Rotational[c] Barrier
3-21G//3-21G	-113.77382	0.78	2.23
6-31G*//6-31G*	-114.40876	1.35	2.78
6-31G**//6-31G**	-114.41912	1.15	2.75
MP2/6-31G**//6-31G*	-114.72369	1.01	4.39
MP2/6-31G**//6-31G**	-114.72352	1.02	4.37
MP3/6-31G**//6-31G*	-114.73935	0.90	3.99
MP3/6-31G**//6-31G**	-114.73922	0.92	3.98

[a] $E(\underset{\sim}{4})$

[b] $E(\underset{\sim}{5}) - E(\underset{\sim}{4})$

[c] $E(\underset{\sim}{6}) - E(\underset{\sim}{4})$

TABLE IV. Theoretical[a] and experimental vibrational frequencies (cm^{-1}) for methanol, methoxy radical and hydroxymethyl radical

Symmetry[b]	Assignment[c]	CH_3OH[d,e] 3-21G	CH_3OH[d,e] 6-31G*	Expt	CH_2OH·[e] 3-21G	CH_2OH·[e] 6-31G*	Expt[f]	CH_3O· 3-21G	CH_3O· 3-21G[g]	CH_3O· 6-31G*	Expt
a'	OH stretch	3868	4117(3705)	3681	3895	4125(3713)	3650	-	-	-	-
	CH_3 d-stretch[h]	3294	3305(2975)	3000	3420	3427(3084)		3254	3274	3255(2930)	
	CH_3 s-stretch[h]	3177	3185(2867)	2844	3280	3289(2960)		3189	3193	3188(2869)	
	CH_3 d-deform[h]	1698	1664(1498)	1477	1619	1626(1463)	1459	1691	1658	1668(1501)	
	CH_3 s-deform[h]	1638	1638(1474)	1455	-	-	-	1584	1579	1585(1427)	1325±30[i]
	OH bend	1479	1508(1357)	1345	1451	1483(1335)	1334	-	-	-	-
	CH_3 rock[h]	1152	1187(1068)	1060	1122	1155(1040)	1048	1158	1239	1225(1103)	
	CO stretch	1092	1164(1048)	1033	1196	1287(1158)	1183	1010	1015	1130(1017)	1015[j]
a"	CH_3 d-stretch[h]	3217	3231(2908)	2960	-	-	-	3277	3256	3274(2947)	
	CH_3 d-deform[h]	1686	1652(1487)	1477	-	-	-	1642	1676	1603(1443)	
	CH_3 rock[h]	1254	1289(1160)	1165	717	850(765)	569	1210	1085	1283(1155)	
	torsion	360	348(313)	295	388	411(370)	420	-	-	-	-

[Footnotes to Table IV]

[a] Theoretical frequencies calculated within the harmonic approximation, i.e. using only the theoretical quadratic force constants.

[b] The symmetry assignments (a' and a") are not strictly valid for $CH_2OH^{\cdot}$ which has $\underline{C}_1$ symmetry.

[c] The most important contribution to the vibrational mode.

[d] From ref. 59.

[h] CH_2 (rather than CH_3) for $CH_2OH^{\cdot}$.

[f] From ref. 13

[i] From ref. 10

[j] From ref. 36

[e] Values scaled by 0.9 shown in parentheses

[g] Values for $^2A"$ state ($\underset{\sim}{3}$) shown for comparison.

TABLE V. Calculated zero-point vibrational energies (HF/3-21G, kcal mol^{-1})

System	ZPVE
$CH_3O^{\cdot}$ ($^2A'$, 2)	25.7
$CH_3O^{\cdot}$ ($^2A''$, 3)	25.7
$CH_2OH^{\cdot}$ (4)	24.5
Inversion TS (5)	23.4
Rotation TS (6)	23.5
Rearrangement TS (7)	21.0
$CH_3O^{\cdot}$ Dissociation TS (8)	18.6
$CH_2OH^{\cdot}$ Dissociation TS (9)	18.6
$CH_2O + H^{\cdot}$	18.2

TABLE VI. Barrier heights[a] and reaction energies (ΔE)[b] (kcal mol^{-1}) for the $CH_3O^{\cdot} \rightarrow CH_2OH^{\cdot}$ unimolecular rearrangement.

Method	Barrier Height[a]	ΔE[b]
3-21G//3-21G	61.7	11.4
6-31G*//6-31G*	56.6	7.5
6-31G**//6-31G**	53.5	4.1
MP2/6-31G**//6-31G*	34.8	-8.8
MP2/6-31G**//6-31G**	34.9	-8.7
MP3/6-31G**//6-31G*	40.2	-4.0
MP3/6-31G**//6-31G**	40.3	-3.8
MP3/6-31G**//6-31G**[c]	36.1	-4.9

[a] Relative to ground state ($^2A'$) $CH_3O^{\cdot}$ ($\underset{\sim}{2}$)

[b] $\Delta E = E(\underset{\sim}{4}) - E(\underset{\sim}{2})$

[c] Value including zero-point vibrational contribution

TABLE VII. Barrier heights (kcal mol^{-1}) for the addition of hydrogen atom to formaldehyde.

Method	$H^{\cdot}+H_2CO \rightarrow H_3CO^{\cdot}$	$H^{\cdot}+H_2CO \rightarrow H_2COH^{\cdot}$
3-21G//3-21G	1.4	7.0
6-31G*//6-31G*	6.1	16.2
6-31G**//6-31G**	5.9	15.4
MP2/6-31G**//6-31G*	16.2	24.2
MP2/6-31G**//6-31G**	16.1	24.3
MP3/6-31G**//6-31G*	12.1	19.6
MP3/6-31G**//6-31G**	12.0	19.7
MP3/6-31G**//6-31G**[a]	12.4	20.1

[a] Value including zero-point vibrational contribution

[FIGURE CAPTIONS]

FIG. 1. Important structural information relating to rearrangement and dissociative processes in the $CH_3O^{\cdot}/CH_2OH^{\cdot}$ potential energy surface. Transition structures are shown in square brackets. Complete structures (with atom numbers as shown) are given in Table I. Bond lengths are HF/6-31G** values, in ångstroms.

FIG. 2. Qualitative view of structures involved in the rotation-inversion surface of $CH_2OH^{\cdot}$. With appropriate labelling, 4a and 4b are enantiomers (optical isomers) while 4a and 4c are synclinal-anticlinal rotational isomers.

FIG. 3. Schematic energy profile (MP3/6-31G**) for rotation-inversion in $CH_2OH^{\cdot}$.

FIG. 4. Schematic potential energy profile for the interconversion and dissociation of $CH_3O^{\cdot}$ (2) and $CH_2OH^{\cdot}$ (4). Relative energies (kcal mol^{-1}) are MP3/6-31G** values together with a zero-point vibrational contribution (see text).

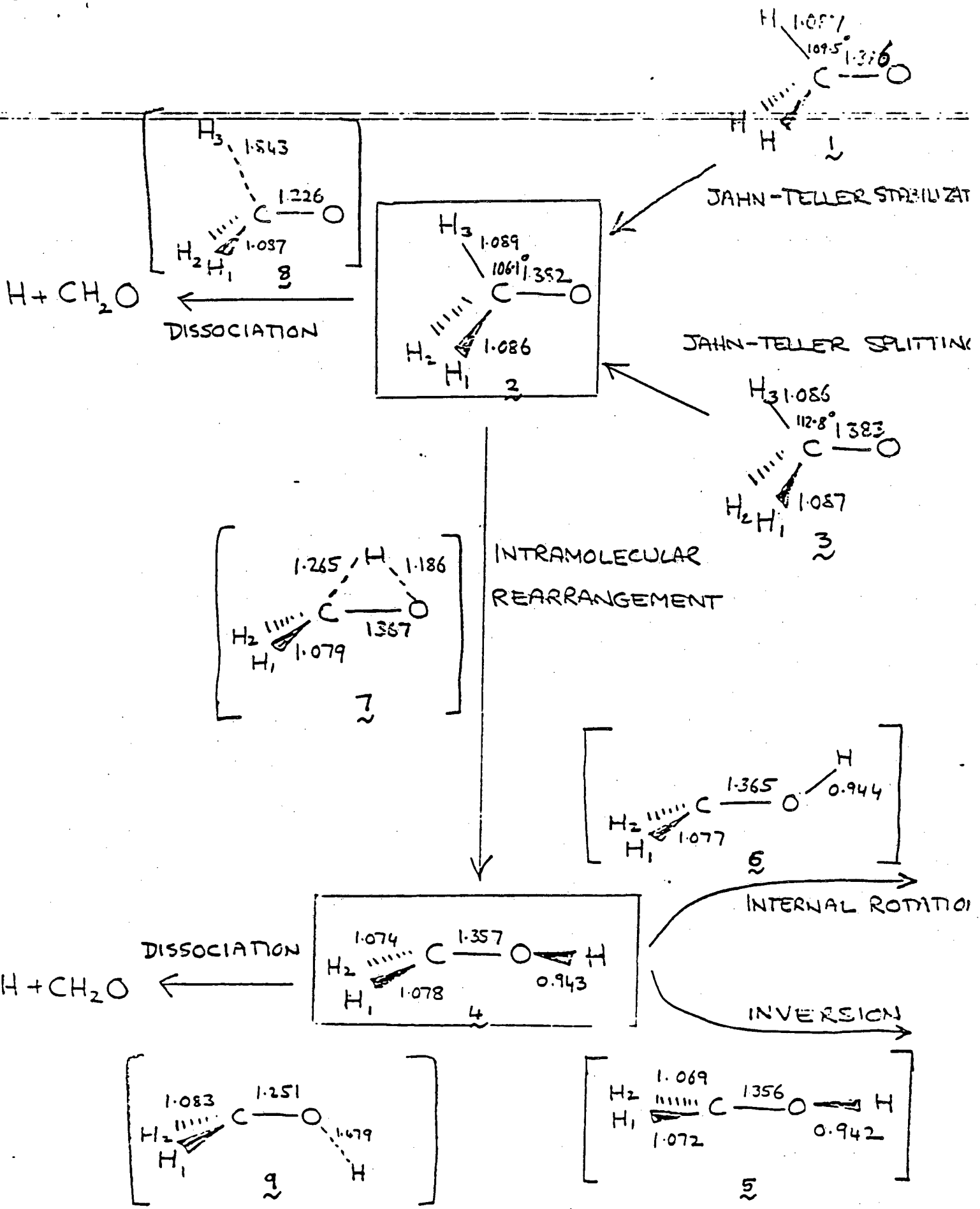
H 1.091
109.5°
1.316
C—O
H H
1
JAHN-TELLER STABILIZAT
H3 1.089
106.1° 1.352
C—O
H2 1.086
H1
2
H3 1.543
1.226
C—O
H2 1.087
H1
8
H + CH2O
DISSOCIATION
JAHN-TELLER SPLITTIN
H3 1.086
112.8° 1.383
C—O
H2 H1 1.087
3
INTRAMOLECULAR
REARRANGEMENT
1.265 H 1.186
C—O
H2 1.367
H1 1.079
7
1.365
H
0.944
C—O
H2 1.077
H1
6
INTERNAL ROTATIO
DISSOCIATION
1.074
1.357
H
C—O
H2 0.943
H1 1.078
4
H + CH2O
INVERSION
1.083
1.251
C—O
H2 1.079
H1 H
9
1.069
H2
H1 C 1.356 O H
1.072 0.942
5

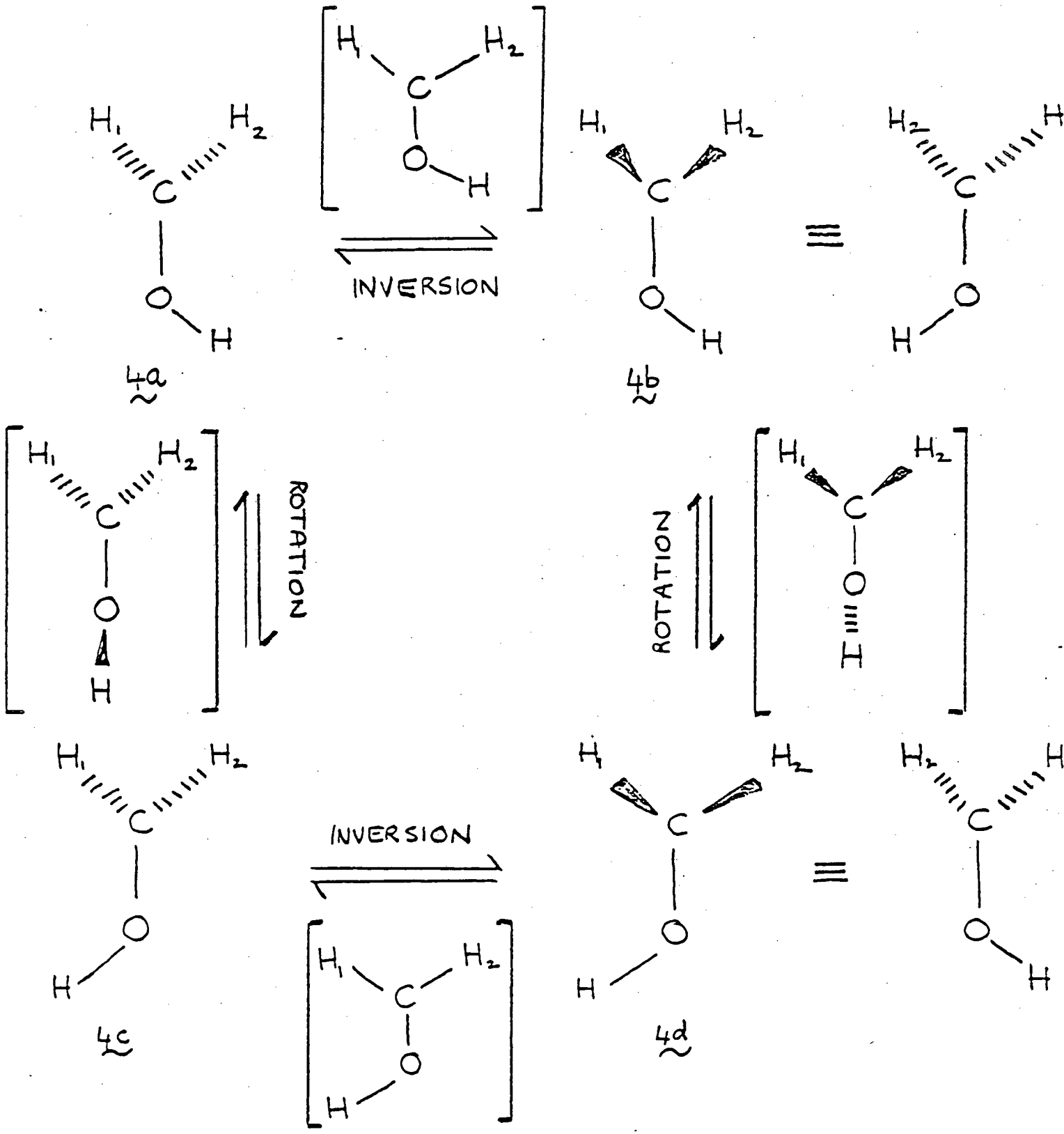

4a 4b 4c 4d

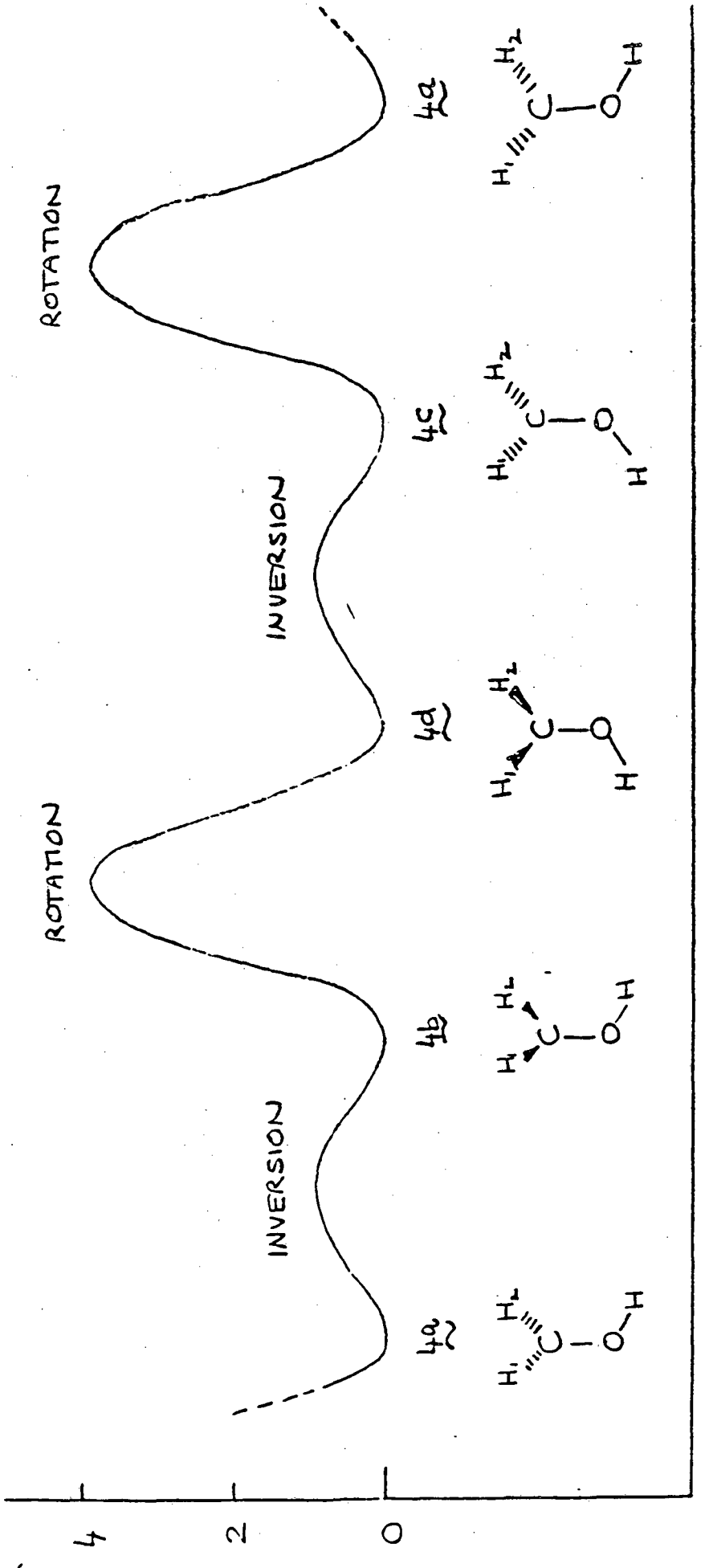
ENERGY (kcal mol⁻¹)
0
2
4
INVERSION
ROTATION
INVERSION
ROTATION
4a
4b
4c
4d
4e

Fig 2

IG. 4

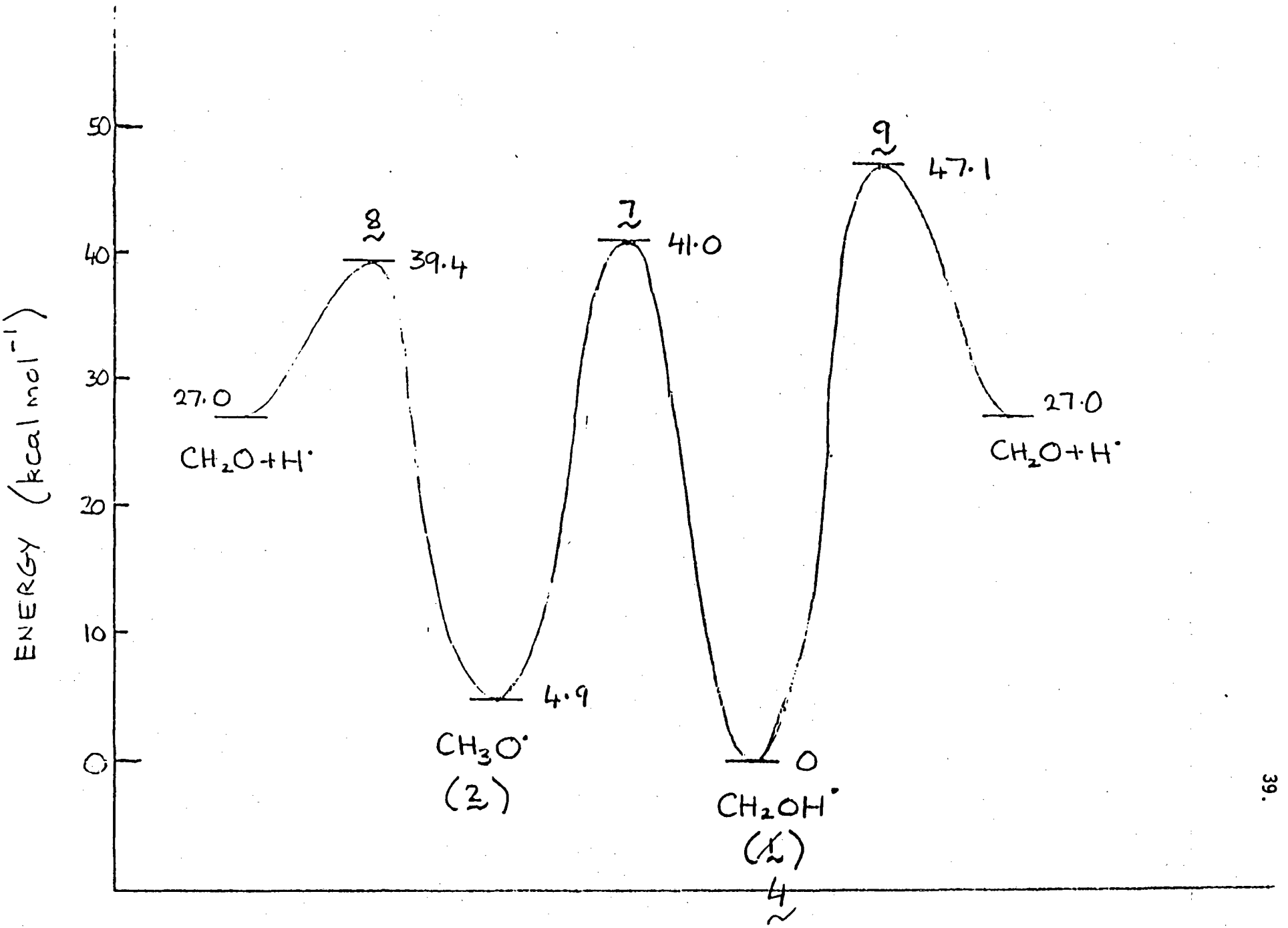
ENERGY (kcal mol⁻¹)
50
40
30
20
10
0
8
39.4
27.0
CH₂O+H·
7
41.0
4.9
CH₃O·
(2)
9
47.1
27.0
CH₂O+H·
0
CH₂OH·
(1)
4

TECHNICAL INFORMATION DEPARTMENT
LAWRENCE BERKELEY LABORATORY
UNIVERSITY OF CALIFORNIA
BERKELEY, CALIFORNIA 94720